

STRUCTURAL BIOLOGY

Structural basis for pH-dependent retrieval of ER proteins from the Golgi by the KDEL receptor

Philipp Bräuer¹, Joanne L. Parker¹, Andreas Gerondopoulos¹, Iwan Zimmermann², Markus A. Seeger², Francis A. Barr^{1*}, Simon Newstead^{1*}

Selective export and retrieval of proteins between the endoplasmic reticulum (ER) and Golgi apparatus is indispensable for eukaryotic cell function. An essential step in the retrieval of ER luminal proteins from the Golgi is the pH-dependent recognition of a carboxyl-terminal Lys-Asp-Glu-Leu (KDEL) signal by the KDEL receptor. Here, we present crystal structures of the chicken KDEL receptor in the apo ER state, KDEL-bound Golgi state, and in complex with an antagonistic synthetic nanobody (sybody). These structures show a transporter-like architecture that undergoes conformational changes upon KDEL binding and reveal a pH-dependent interaction network crucial for recognition of the carboxyl terminus of the KDEL signal. Complementary *in vitro* binding and *in vivo* cell localization data explain how these features create a pH-dependent retrieval system in the secretory pathway.

In eukaryotic cells, millimolar levels of chaperones required for protein folding in the endoplasmic reticulum (ER) are discriminated from newly synthesized secretory and membrane proteins which pass through the ER on their way to the Golgi apparatus (1). Luminal chaperones and ER-resident membrane proteins carry a C-terminal Lys-Asp-Glu-Leu (KDEL) sequence required for retention in the ER (2). When these proteins escape to the Golgi, they are recognized by an integral membrane protein, the KDEL receptor (KDELRL), and retrieved back to the ER (3). The retrieval receptor ERD2 was discovered in 1990 as one of a number of ER retention defective (ERD) mutants in *Saccharomyces cerevisiae* (3–5). *ERD2* encodes the 26-kDa KDELRL that enables yeast to retain ER luminal chaperones (3). It is predicted to have seven transmembrane domains and belongs to a large and diverse family of membrane proteins called the PQ-loop superfamily, which play important roles in lysosomal transport, tissue development, and nutrient transport in plants and bacteria (6). The KDELRL is localized to the cis-Golgi, where it can efficiently capture escaped ER luminal proteins (7, 8). The interaction with KDEL proteins is pH-sensitive, with maximal binding below pH 6 (9). The luminal pH of the cis-Golgi is 6.2, whereas that of the ER lumen is 7.2 to 7.4 (10, 11), explaining how the KDELRL could bind and release KDEL-carrying proteins in these organelles, respectively. Binding of a protein with a KDEL sequence to the receptor triggers incorporation of the complex into COPI vesicles, resulting in return of the complex to the ER (12). Once there, the complex dissociates and the receptor is rapidly

trafficked back to the Golgi via COPII vesicles (13, 14). The cytoplasmic surface of the KDELRL is thought to mediate the interaction with the COPI vesicle machinery, although how this mediation occurs or how it is coupled to KDEL binding remains unknown (13, 14). To elucidate the molecular basis for receptor-mediated retrieval in the secretory pathway, we determined the crystal structure of the KDELRL in both the peptide-free and -bound states.

To determine the atomic structure of the KDELRL, we screened several homologs from different eukaryotic sources to identify a receptor suitable for structural and biophysical characterization. *Gallus gallus* KDELRL2 displays the characteristic pH-dependent binding for the KDEL peptide in the absence of any additional cofactors, with a dissociation constant of $1.25 \pm 0.14 \mu\text{M}$ at pH 5.0 in detergent (Fig. 1A). Binding of the peptide is calcium independent (fig. S1), suggesting luminal calcium plays no role in the retrieval cycle. The structure was determined to 2.5-Å resolution at pH 9.0 in the peptide-free apo state (table S1). The structure has similarities to the eukaryotic SWEET transporter (15) (fig. S2), despite sharing only 24% sequence identity, and does not resemble the G protein-coupled receptor family of cell surface receptors. The receptor adopts a compact structure, consisting of seven transmembrane (TM) alpha helices arranged loosely in a hexagonal configuration when viewed from above (Fig. 1B). The first three N- and last three C-terminal helices form two internal triple helix bundles (THBs) arranged in a 1-3-2 sequence, connected with inverted topology by the linker helix TM4. This structural arrangement, whereby the THBs are inverted relative to each other by a pseudo two-fold rotation axis in the plane of the membrane (fig. S3), suggests an evolutionary relationship to secondary active transporters (6).

The surface of the cytosolic face contains a prominent central band of negative charge running down its center (Fig. 1C). The negative charge is contributed by several acidic residues invariant in the mammalian KDELRLs: Asp⁵⁷, Glu¹⁴³, Glu¹⁴⁵, and the C terminus of TM7 (figs. S4 and S5). Cell biological studies identified these and several additional residues in the cytoplasmic portion of human KDELRL (*ERD2.1*) that result in retention within the ER when mutated (16). Many of these residues function to support the structural integrity of this electrostatic feature, suggesting this feature may form part of a diacidic COPII-binding ER-exit motif (17). The hydrophobic surface of the receptor is noticeably short, measuring 27 Å at its widest point (Fig. 1D), which is consistent with other membrane proteins resident in thin membrane bilayers of the ER and Golgi (18, 19). The asymmetric position of this narrow hydrophobic belt suggests that the receptor projects outward from the cytosolic side of the membrane, exposing the negatively charged surface. Likewise, the receptor would be flush with the luminal side of the ER and Golgi membranes, where it recognizes KDEL-containing proteins. A large polar cavity is observed at the luminal side of the receptor, flanked by side chains from TMs 1 to 3 from the N-terminal THB and TMs 5 to 7 from the C-terminal THB, and measuring 13 Å by 15 Å by 12 Å (Fig. 1E). The electrostatic surface of the cavity is charged, with a pronounced dipolar character contributed by Arg⁵ (TM1) and Arg¹⁶⁹ (TM6), which are positioned opposite Glu¹¹⁷ (TM5) and Asp¹⁷⁷ (TM7) (fig. S6). As discussed later, these residues form an integral part of the KDEL signal sequence recognition site.

Binding of the KDEL signal sequence to the human receptor is pH-dependent, yet the mechanism through which high-affinity binding depends on acidic pH is unclear (9, 20). To address this question, we determined, to a resolution of 2.0 Å, a second structure of the *G. gallus* KDELRL2 bound to the Thr-Ala-Glu-Lys-Asp-Glu-Leu (TAEKDEL) peptide at an acidic pH of 6.0 (table S1). The TAEKDEL peptide bound in the luminal-facing cavity adopts a vertical orientation with respect to the membrane, with the AEKDEL residues clearly resolved in the electron density map (Fig. 2A and fig. S7). Compared to the apo form, the peptide-bound receptor shows rearrangement of the side chains and helices forming the luminal-facing cavity (Fig. 2B and fig. S8). The cytoplasmic half of TM6 rotates inward, which results in Arg¹⁵⁹ moving ~4.8 Å toward the peptide. This allows the C terminus of the KDEL ligand to be anchored in place through two salt bridge interactions to Arg¹⁵⁹ (TM6) and Arg⁴⁷ (TM2) (Fig. 2B). In this conformation, the luminal half of TM1 has moved outward to accommodate the peptide, with Arg⁵ adopting a new rotamer configuration to interact with a carbonyl group on the peptide. Movement of TM1 also creates a pocket that accommodates the leucine side chain of the KDEL sequence. Recognition of the remaining side chains is predominantly mediated through electrostatic interactions to the sides of the

¹Department of Biochemistry, University of Oxford, South Parks Road, Oxford OX1 3QU, UK. ²Institute of Medical Microbiology, University of Zurich, 8006 Zurich, Switzerland. *Corresponding author. Email: simon.newstead@bioch.ox.ac.uk (S.N.); francis.barr@bioch.ox.ac.uk (F.A.B.)

luminal-facing cavity. The positive amine group of the lysine interacts with Glu¹¹⁷ (TM5) in a negatively charged pocket (Fig. 2C). The aspartate of the KDELR sequence makes a salt bridge to Arg¹⁶⁹ (TM6), whereas the glutamate interacts via a third salt bridge to Arg⁵ (TM1) and makes a hydrogen bond interaction to Trp¹⁶⁶, which, similarly to Arg¹⁵⁹, moves inward to engage the peptide during the movement of TM6. The KDELR shows maximal binding between pH 5.0 and 5.4 with a gradual reduction in affinity until pH 7.0 (Fig. 1A). Our structures reveal that repositioning of TM6 upon peptide binding is stabilized through the formation of a short hydrogen bond, measuring ~2.5 Å, between Tyr¹⁵⁸ (TM6) and Glu¹²⁷ (TM5) (Fig. 2D and fig. S9). Formation of this short hydrogen bond would stabilize the new position of TM6, locking the peptide in place through its interaction with Arg¹⁵⁹. Tyr¹⁵⁸ sits close to a strictly conserved histidine on TM1, His¹², forming an aromatic interaction. Two water molecules sit at the bottom of the peptide-binding site, coordinating the peptide carboxyl group to both Tyr¹⁵⁸ and His¹², which are further stabilized through a hydrogen bond to Asp⁹ on TM1 (Fig. 2D and movie S1). Given its solvent-accessible position within the peptide-binding site, it is possible

that protonation of His¹² facilitates the formation of the short hydrogen bond that stabilizes the repositioning of TM6, and thus acts as the pH sensor within the receptor. Supporting this proposal, conservative mutations in these residues resulted in the loss of KDELR binding in vitro (Fig. 3A). The loss of binding to the chicken receptor in vitro was matched by a failure of equivalent variants of the human receptor (ERD2.1) to respond to KDELR ligand overexpression in vivo, with the receptor remaining localized in the Golgi despite the presence of KDELR ligand (Fig. 3, B and C). Mutation of Arg¹⁵⁹ (TM6) resulted in a ligand-binding-defective protein trapped in the ER (Fig. 3, A to C), suggesting this residue is important for the conformational stability of the receptor.

In the peptide-bound structure, we also observed a pronounced effect at the cytoplasmic surface of the receptor, with TM7 moving away from TM5, ~14 Å relative to the apo receptor, and creating a new cavity facing the cytoplasm (Fig. 4, A and B). This movement results in the repositioning of a strictly conserved acidic residue, Asp¹⁹³ (TM7). Although an Asp¹⁹³→Asn mutant in the human receptor was previously shown to bind KDELR peptide in vitro (16), our data show this variant remains trapped in the Golgi in vivo,

even in the presence of an excess of KDELR ligand (Fig. 4, C and D). This supports the view that movement of TM7 and opening of the cytosol-facing cavity is important for ER retrieval via COPI. Consistent with this hypothesis, the movement of TM7 exposes a cluster of lysine residues (Lys²⁰¹, Lys²⁰⁴, and Lys²⁰⁶) buried in the apo receptor (Fig. 4A) that could form an ER-retrieval motif (21, 22). Additionally, the movement of TM6, discussed in relation to peptide binding above, causes the peptide chain linking TM5 and TM6 to shorten, as the length of TM6 is extended by one helical turn at the cytoplasmic end (fig. S10). This rearrangement results in the central band of negative charge, which was a prominent feature of the cytoplasmic face of the apo receptor, to lengthen and split into two equal regions (Fig. 4C). It is likely that such a drastic change in the electrostatics on the cytosolic-facing surface of the receptor plays a role in mediating the interaction between the KDELR and the COPI and COPII coatomer complexes during receptor trafficking. As already noted, the exposed lysine cluster on TM7 is similar to previously observed KKXX and KKKXX dilysine motifs, which are important in COPI-dependent Golgi-to-ER transport (21, 22). To test their importance in the human KDELR, we mutated this motif and observed that the

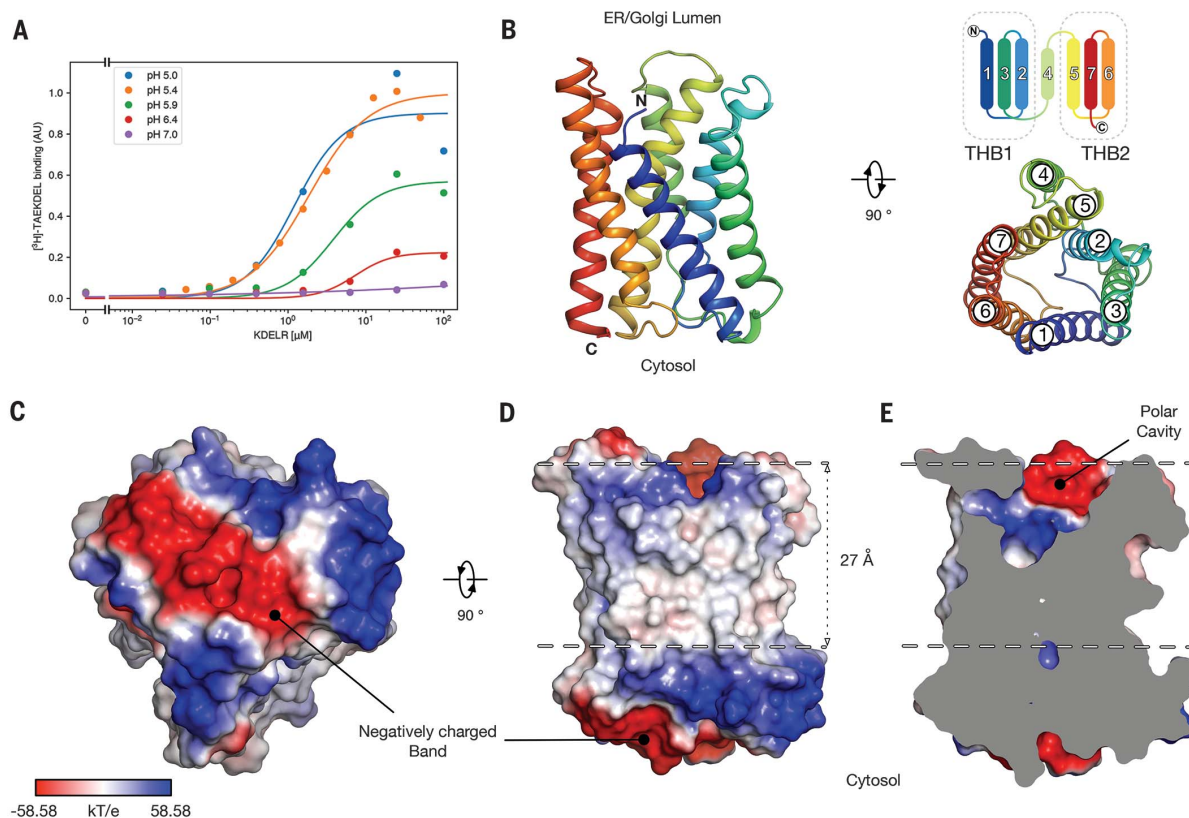


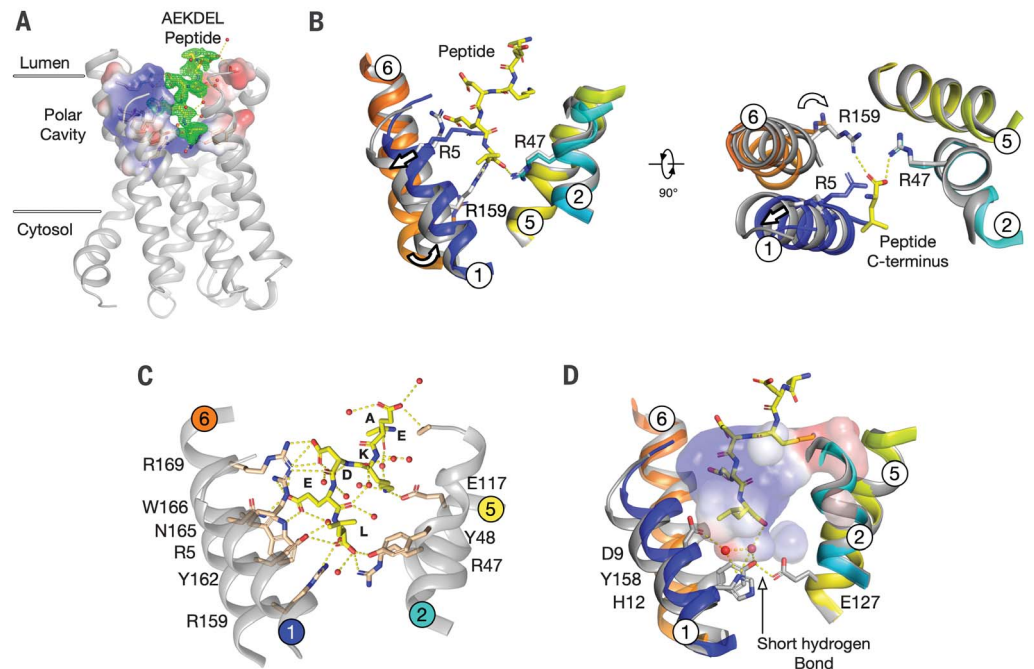
Fig. 1. Crystal structure of the KDELR. (A) Representative curves showing normalized binding of [³H]-TAEKDEL peptide to the KDELR at different pH conditions. (B) Crystal structure of KDELR viewed from the Golgi membrane. The transmembrane helices are labeled by number. (Top right) Topology of the fold, highlighting the two triple helix bundles (THB1

and THB2). (C) Electrostatic surface representation of KDELR highlighting the negatively charged band on the cytosolic side of the receptor. (D) View in (A) rotated 90°, showing placement of the receptor with respect to the membrane bilayer (dashed lines). (E) Sliced-through volume representation of (D), highlighting the polar cavity on the luminal side of the receptor.

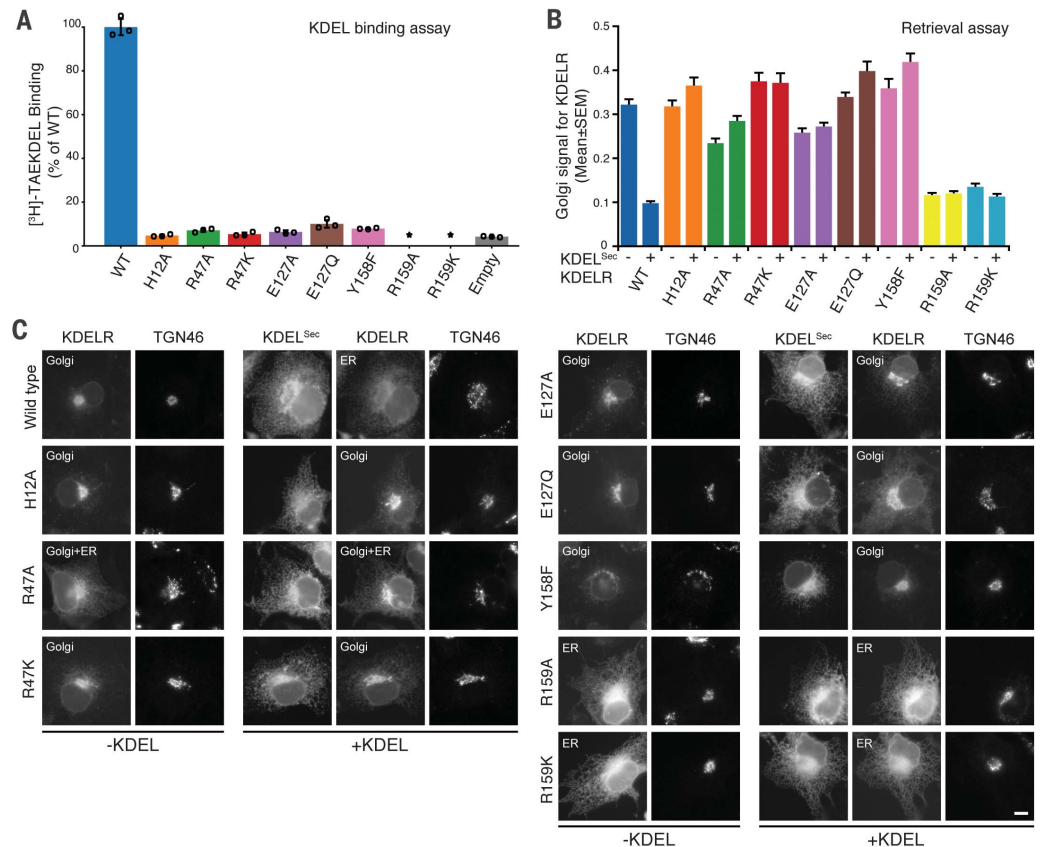
Fig. 2. Molecular basis for KDEL peptide recognition.

(A) The polar cavity in KDEL_R is shown with contributing side chains represented as sticks and their electrostatic surface shown. The bound TAEKDEL peptide is shown with the *mFo-DFc* difference electron density (green mesh) used for model building displayed, contoured at 3 σ . The N-terminal threonine was disordered in the maps and not modeled. Water molecules are represented as spheres (red) with hydrogen bonds as dashed lines (yellow).

(B) Close-up view of the polar cavity showing the structural movement induced in TM1 and TM6 upon peptide binding. The apo structure is shown in colored helices, the peptide-bound structure in gray. In the top-down view (right), only the C-terminal leucine of the peptide is shown. **(C)** Close-up view of the polar cavity shown in (A). Water molecules are represented as spheres (red) with hydrogen bonds as dashed lines (yellow). **(D)** Overlay of the apo (color-coded helices) and peptide-bound structure (gray), highlighting the short hydrogen bond formed between Glu¹²⁷ and Tyr¹⁵⁸ at the base of the polar cavity after peptide binding. Two water molecules coordinate the interaction between the C terminus of the peptide with Tyr¹⁵⁸ and His¹². Single-letter abbreviations for the amino acid residues are as follows: A, Ala; C, Cys; D, Asp; E, Glu; F, Phe; G, Gly; H, His; I, Ile; K, Lys; L, Leu; M, Met; N, Asn; P, Pro; Q, Gln; R, Arg; S, Ser; T, Thr; V, Val; W, Trp; and Y, Tyr.

**Fig. 3. Functional characterization of binding-site mutations.**

(A) In vitro binding assay using purified chicken KDEL_R. Asterisk indicates protein that could not be produced. **(B)** ER retrieval assays were performed in the absence (–) or presence (+) of KDEL^{Sec} and the Golgi signal for KDEL_R is plotted as mean \pm SEM. **(C)** KDEL_Rs were tested for KDEL^{Sec}-induced redistribution from Golgi to ER as in (B). TGN46 was used as a Golgi marker. Scale bar, 10 μ m.



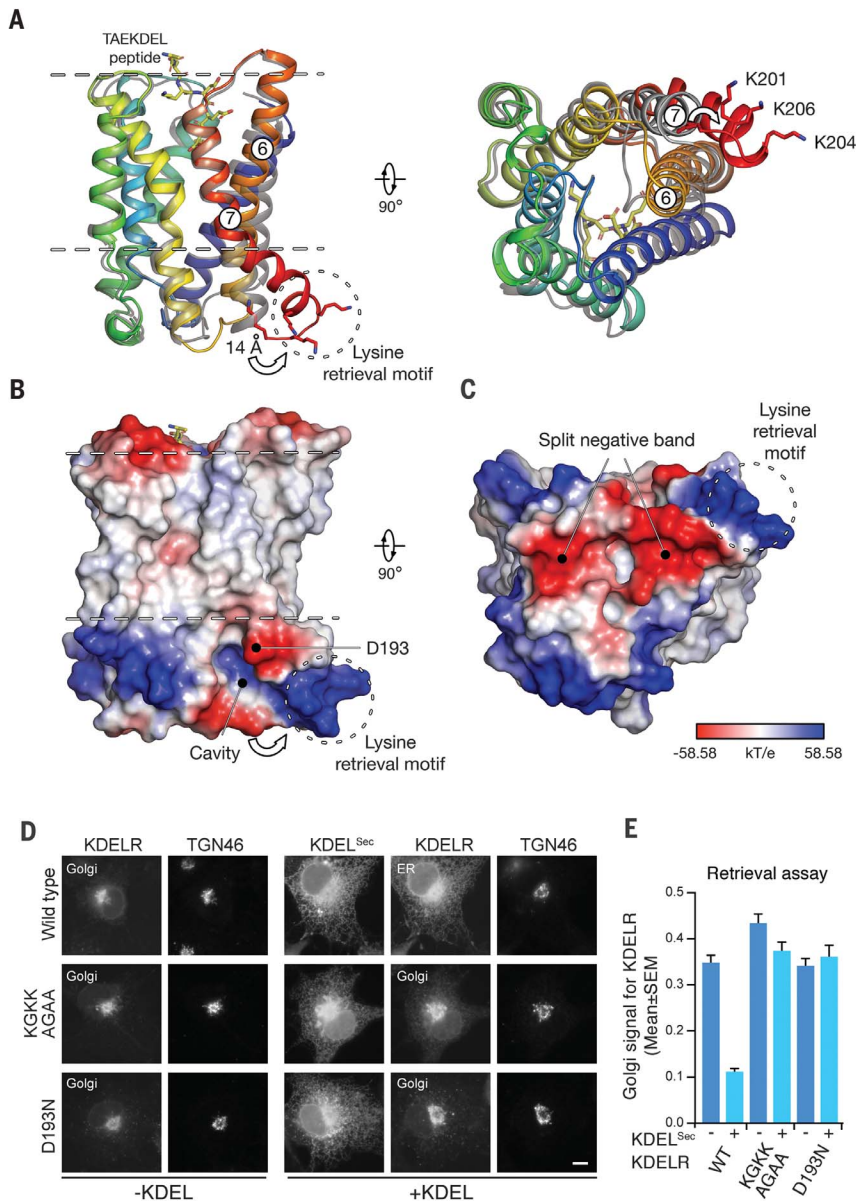


Fig. 4. Structural basis for exposure of COPI retrieval signal. (A) Overlay of the apo (gray) and peptide-bound (colored helices) crystal structures of the KDEL receptor. The movement of TM7 is highlighted, exposing the C-terminal lysine side chains, indicated by the dashed circle. (Right) Cytoplasmic view of the receptor with the movement in TM7 indicated. (B) Electrostatic surface representation of (A). Dashed lines indicate rough position of the Golgi membrane, and the lysine retrieval motif is indicated by the dashed circle. After movement of TM7, a new cavity opens on the cytoplasmic side of the receptor, exposing Asp¹⁹³. (C) Cytoplasmic surface of the receptor, showing the substantial change in distribution of surface charge, most notably the disruption of the negative band present in the apo state. (D) Wild-type, Asp¹⁹³→Asn, and KGKK-dilysine motif mutant KDEL receptors were tested for KDEL^{Sec}-induced redistribution from Golgi to ER. TGN46 was used as a Golgi marker. Scale bar, 10 μ m. (E) Golgi signal for KDEL in retrieval assays performed as in (D), in the absence (–) or presence (+) of KDEL^{Sec} is plotted as mean \pm SEM.

protein remained localized in the Golgi upon KDEL ligand overexpression (Fig. 4, D and E). This motif therefore plays an important role during KDEL-mediated ER retrieval.

In the course of determining the crystal structure, we employed synthetic nanobodies, or

sybodies, generated using an in vitro selection platform (23). A crystal structure, obtained at 2.23-Å resolution in the absence of KDEL peptide (table S1), demonstrates that the CDR3 loop of the sybody binds within the luminal-facing cavity yet fails to induce the movement of either TM6 or

TM7 (fig. S11, A to E). Using a version of Syb37 targeted to the Golgi lumen, Syb37^{Sec}, we observed partial redistribution of KDEL receptor–Syb37^{Sec} complexes from the Golgi to LAMP1-positive structures (fig. S11F). These results are consistent with the receptor no longer undergoing normal signal-mediated retrieval from the Golgi, but instead following the bulk flow pathway to the lysosome. Importantly, Syb37^{Cyto}, a cytoplasmic version unable to access the Golgi lumen, did not have this effect. The inability of the sybody to activate the KDEL receptor either in vitro or in vivo highlights the importance of the specific interactions with the peptide in the luminal-facing cavity and subsequent movements in TM6 and TM7 that, we propose, define two conformations of the KDEL receptor, which are important for anterograde and retrograde trafficking, respectively.

Taken together, our data support a mechanism whereby changes in the electrostatics on the cytoplasmic surface of the receptor, in combination with protonation of a key histidine and peptide binding, play an important role in retrieval of the receptor via the COPI pathway (fig. S12). A notable discovery from this work is the presence of mutually exclusive basic COPI and putative acidic patch COPII recognition motifs. TM7 plays a pivotal role in presenting these motifs. The structural change in TM7 is stabilized by an interaction network involving a conserved histidine located adjacent to the KDEL signal sequence binding pocket. This creates an elegant way for the KDEL receptor to switch between the COPII ER-to-Golgi and COPI Golgi-to-ER trafficking pathways in a pH-dependent manner.

REFERENCES AND NOTES

1. L. Ellgaard, A. Helenius, *Nat. Rev. Mol. Cell Biol.* **4**, 181–191 (2003).
2. S. Munro, H. R. Pelham, *Cell* **48**, 899–907 (1987).
3. J. C. Semenza, K. G. Hardwick, N. Dean, H. R. Pelham, *Cell* **61**, 1349–1357 (1990).
4. F. M. Townsley, G. Frigerio, H. R. Pelham, *J. Cell Biol.* **127**, 21–28 (1994).
5. H. R. Pelham, K. G. Hardwick, M. J. Lewis, *EMBO J.* **7**, 1757–1762 (1988).
6. L. Feng, W. B. Frommer, *Trends Biochem. Sci.* **41**, 118–119 (2016).
7. M. J. Lewis, H. R. Pelham, *Cell* **68**, 353–364 (1992).
8. G. Griffiths *et al.*, *J. Cell Biol.* **127**, 1557–1574 (1994).
9. D. W. Wilson, M. J. Lewis, H. R. Pelham, *J. Biol. Chem.* **268**, 7465–7468 (1993).
10. M. M. Wu *et al.*, *Chem. Biol.* **7**, 197–209 (2000).
11. M. M. Wu *et al.*, *J. Biol. Chem.* **276**, 33027–33035 (2001).
12. I. Majoul, M. Straub, S. W. Hell, R. Duden, H. D. Söling, *Dev. Cell* **1**, 139–153 (2001).
13. S. R. Pfeffer, *Annu. Rev. Biochem.* **76**, 629–645 (2007).
14. N. Gomez-Navarro, E. Miller, *J. Cell Biol.* **215**, 769–778 (2016).
15. Y. Tao *et al.*, *Nature* **527**, 259–263 (2015).
16. F. M. Townsley, D. W. Wilson, H. R. Pelham, *EMBO J.* **12**, 2821–2829 (1993).
17. C. Barlowe, *Trends Cell Biol.* **13**, 295–300 (2003).
18. H. J. Sharpe, T. J. Stevens, S. Munro, *Cell* **142**, 158–169 (2010).
19. J. L. Parker, S. Newstead, *Nature* **551**, 521–524 (2017).
20. A. A. Scheel, H. R. Pelham, *J. Biol. Chem.* **273**, 2467–2472 (1998).
21. F. Letourneur *et al.*, *Cell* **79**, 1199–1207 (1994).
22. L. P. Jackson *et al.*, *Dev. Cell* **23**, 1255–1262 (2012).
23. I. Zimmermann *et al.*, *eLife* **7**, e34317 (2018).

ACKNOWLEDGMENTS

We thank the staff of beamlines I24 Diamond Light Source, UK, for assistance. **Funding:** This work was supported by Wellcome awards (102890/Z/13/Z, 109133/Z/15/A, and 097769/Z/11/Z) to S.N. and F.A.B. and SNSF Professorship of the Swiss National Science Foundation (PP00P3_144823) and Commission for Technology and Innovation CTI (16003.1 PFLS-LS) to M.A.S. **Author contributions:** S.N., J.L.P., M.A.S., and F.A.B. designed the experiments and interpreted the data. P.B., J.L.P., A.G., I.Z., and S.N. carried out the experiments

and interpreted the data. P.B., J.L.P., F.A.B., and S.N. wrote the paper. **Competing interests:** The authors declare no competing interests. **Data and materials availability:** Atomic coordinates for the models have been deposited in the Protein Data Bank under accession codes 6I6J (Syb37-KDEL2 complex), 6I6B (Apo structure), and 6I6H (peptide-bound structure). Expression plasmids containing the cloned genes detailed in this study are available from Addgene under a material agreement with the University of Oxford.

SUPPLEMENTARY MATERIALS

www.sciencemag.org/content/363/6431/1103/suppl/DC1
Materials and Methods
Figs. S1 to S14
Table S1
References (24–35)
Movie S1

5 December 2018; accepted 13 February 2019
10.1126/science.aaw2859

Structural basis for pH-dependent retrieval of ER proteins from the Golgi by the KDEL receptor

Philipp Bräuer, Joanne L. Parker, Andreas Gerondopoulos, Iwan Zimmermann, Markus A. Seeger, Francis A. Barr and Simon Newstead

Science **363** (6431), 1103-1107.
DOI: 10.1126/science.aaw2859

Crystal structure of the KDEL receptor

Eukaryotic cells concentrate chaperones in the lumen of the endoplasmic reticulum (ER). These chaperones can be swept along the secretory pathway to the Golgi apparatus, from where they must be returned. For 20 years, cell biologists have known the identity of the KDEL (Lys-Asp-Glu-Leu) receptor responsible for this process, but the molecular basis for its function has remained elusive. Now, Bräuer *et al.* present crystal structures of the KDEL receptor, in both the apo ER state and KDEL retrieval signal –bound Golgi state. Comparisons of these two states identify the conformational switch that exposes the ER retrieval motif. The authors recapitulated the binding and release cycle of the receptor using purified components, confirming that the receptor is the minimal component required to bind KDEL ligands in the Golgi.

Science, this issue p. 1103

ARTICLE TOOLS

<http://science.sciencemag.org/content/363/6431/1103>

SUPPLEMENTARY MATERIALS

<http://science.sciencemag.org/content/suppl/2019/03/06/363.6431.1103.DC1>

REFERENCES

This article cites 35 articles, 6 of which you can access for free
<http://science.sciencemag.org/content/363/6431/1103#BIBL>

PERMISSIONS

<http://www.sciencemag.org/help/reprints-and-permissions>

Use of this article is subject to the [Terms of Service](#)

Science (print ISSN 0036-8075; online ISSN 1095-9203) is published by the American Association for the Advancement of Science, 1200 New York Avenue NW, Washington, DC 20005. The title *Science* is a registered trademark of AAAS.

Copyright © 2019 The Authors, some rights reserved; exclusive licensee American Association for the Advancement of Science. No claim to original U.S. Government Works